Interpreting AVO Anomalies

D. J. Foster, **Atlantic Richfield Co.**

Summary

We investigated the effects of changes in rock properties on AVO responses. In the slope-intercept domain, reflections from wet sands and shales fall on a trend, the Fluid Line. Reflections from the tops of sands containing gas or light hydrocarbons fall on a trend below the Fluid Line; reflections from the base of gas sands fall on a trend above the Fluid Line. The distance of these trends from the Fluid Line depends upon pore fluid compressibility; i.e., distance increases with increasing compressibility. But, if all other factors are equal, base of sand reflections are displaced further from the Fluid Line than top of sand reflections. Consequently, base of sand reflections, which identify down-dip limits and fluid contacts, will be more prominent than top of sand reflections. Porosity changes affect acoustic impedance, but do not significantly impact the *Vp/Vs* contrast. As a result, porosity changes move the AVO response along trends parallel to the Fluid Line.

Effects of Elastic Property Changes on AVO

For small angles of incidence θ, usually less than 30°, Shuey (1985) and others have shown that the compressional wave reflection coefficient is approximately

$$R(\theta) = A + B\sin^2(\theta) \quad (1)$$

In (1), θ is the angle of incidence, A is the intercept or value of the reflection coefficient at normal incidence, and B is the slope, which measures amplitude increase or decrease with incidence angle or offset.

For small perturbations in velocity and density at a reflecting interface, the intercept and slope may be approximated by (Aki and Richards, 1980)

$$A = \frac{\Delta\alpha}{2\alpha} + \frac{\Delta\rho}{2\rho} \text{ and} \quad (2)$$

$$B = \frac{\Delta\alpha}{2\alpha} - 4\frac{\beta^2}{\alpha^2}\left\{\frac{\Delta\rho}{2\rho} + \frac{\Delta\beta}{\beta}\right\}. \quad (3)$$

In (2) and (3), α, β, and ρ are the averages of the compressional wave velocity (*Vp*), shear wave velocity (*Vs*), and density above and below the reflecting interface; $\Delta\alpha$, $\Delta\beta$, and $\Delta\rho$ are the differences in compressional wave velocity, shear wave velocity, and density between the layer below and the layer above the reflector.

Let $\gamma = \beta/\alpha$. Neglecting second order terms,

$$\frac{\Delta\gamma}{\gamma} = \frac{\Delta\beta}{\beta} - \frac{\Delta\alpha}{\alpha}. \quad (4)$$

Substituting (4) into (3) and collecting terms shows that

$$B = (1-8\gamma^2)A - 4\gamma\Delta\gamma + (4\gamma^2 - 1)\frac{\Delta\rho}{2\rho}.$$

If the ratio γ is close to ½, the last term can be neglected as a second order perturbation, yielding the equation

$$B = (1-8\gamma^2)A - 4\gamma\Delta\gamma. \quad (5)$$

Equation (5) describes a family of lines that are parallel to the line

$$B = (1-8\gamma^2)A. \quad (6)$$

See Figure 1. We call the line defined by (6) the "Fluid Line". The slope of the Fluid Line depends on the background *Vp/Vs* ratio (*Vp/Vs* = 1/γ). The slope of the Fluid Line is –1 if *Vp/Vs=2* (γ=½) and the Fluid Line trend rotates counterclockwise as background *Vp/Vs* increases.

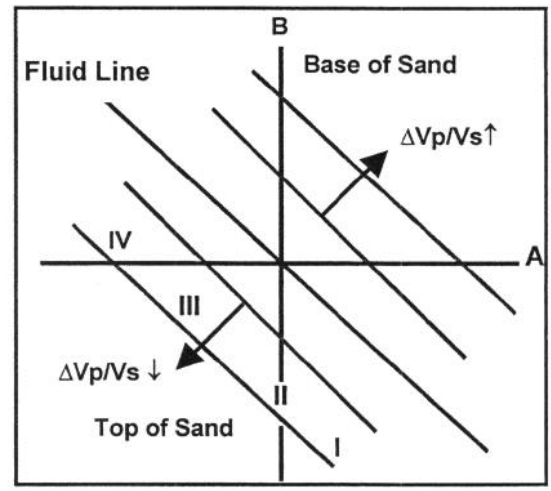

Figure 1. Intercept (A) vs. Slope (B) Cross Plot. AVO responses at top of sand are shown for the four classes of gas sands

These observations about the Fluid Line hold whether the background Vp/Vs is constant or slowly varying (Castagna, et al., 1998).

The Fluid Line is important because reflections from wet sands and shales, which have little contrast in *Vp/Vs*, tend to fall on the Fluid Line trend; reflections from hydrocarbon bearing sands do not.

From (5), an abrupt decrease in *Vp/Vs* will cause the slope-intercept pair to fall on a trend below the Fluid Line trend. The new trend is displaced from the Fluid Line by an amount proportional to the change in *Vp/Vs*, $-4\gamma\Delta\gamma$. Since gas or light hydrocarbons cause an abrupt decrease in the *Vp/Vs* ratio of a porous sand, reflections from the tops of hydrocarbon bearing sands fall on a trend below the Fluid Line.

Similarly, the abrupt increase in *Vp/Vs* at the base of a hydrocarbon bearing sand will position the slope-intercept pair on a trend above the Fluid Line. Reflections from the base of hydrocarbon bearing sands fall on trends above the Fluid Line.

Rutherford and Williams (1989) identified three classes of AVO responses based on acoustic impedance contrasts. Castagna and Swan (1997) added a fourth class of gas sands that appear as a "bright spots" on true-amplitude processed seismic data. Figure 1 depicts the AVO response of reflections from the tops of the four classes of gas sands. The relationship between these AVO classes is easily explained with Equation (5).

Note that the four classes of gas sands are aligned on a trend in Figure 1. This is intentional. Using an equation similar to (5), Batzle, Han, and Castagna (1995) showed that the *Vp/Vs* contrast depends on the type of pore fluid. Therefore, the AVO response of the four classes of gas sands must fall on the trend that corresponds to the *Vp/Vs* contrast for gas sands. Their position on the gas sand trend depends on their acoustic impedance contrast with the surrounding rocks. The reflection coefficient intercept is a measure of impedance contrast.

A Class I gas sand has higher acoustic impedance than the encasing shale. Equation (5) shows that a reflection from the top of a Class I gas sand must lie below the Fluid Line trend, to the right of the slope axis. Therefore, the reflection from the top of a Class I gas sand is positive at normal incidence, but decreases with increasing offset faster than background reflections.

If the acoustic impedance of the gas sand is reduced to that of the surrounding shale, it becomes a Class II gas sand. An increase in porosity can cause this reduction in acoustic impedance. The slope-intercept point for a Class II gas sand lies at the intersection of the gas sand trend with the slope axis. The reflection from the top of a Class II gas sand is negligible at zero-offset, but has a large negative slope, so that its amplitude becomes large and negative with increasing offset.

Reducing acoustic impedance (increasing porosity) further leads to a Class III gas sand that has lower impedance than the overlying shale. Figure 1 shows that the reflection from the top of a Class III gas sand has negative intercept and slope. A reflection from the top of a Class III gas sand is negative at normal incidence, and becomes more negative with increasing offset.

Continuing to decrease the acoustic impedance produces a Class IV gas sand or bright spot. Figure 1 shows that a Class IV has negative intercept, but slope is zero or positive. The reflection from the top of a Class IV gas sand is large and negative, but its magnitude does not increase with offset.

Exact A's and B's

Equation (5) was based on approximations for slope and intercept that assumed small perturbations in elastic properties at the reflecting interface. While these approximations are adequate for modeling the offset-dependent behavior of the compressional wave reflection coefficient, are they accurate enough to describe the relationship between intercept and slope? What are the consequences of neglecting second order perturbations on Equation (5)?

Exact equations for slope and intercept based on the Zoeppritz equations (Achenbach, 1973, p. 186) are given by Foster, Keys, and Schmitt (1997, p. 199). For general media, these equations are too complicated to transform into a relation between slope and intercept like (5). However, a relation between slope and intercept can be derived for special cases. In particular, if we assume that density does not vary across the reflecting interface, then the exact intercept and slope satisfy the equation

$$B = (1-8\gamma^2)A - 4\gamma\Delta\gamma(1-\Delta\gamma) + (1-2\gamma)O(A^2). \quad (7)$$

In (7), second order perturbations are retained, but third order and higher perturbations are neglected. Although (7) assumes constant density, exact slope and intercept values calculated from sonic and density logs match trends predicted by Equation (7) very well. (See Figure 3.)

There are two obvious differences between (5) and (7). These differences have practical significance. First, the error term in (7) shows that second order perturbations in A vanish when $\gamma = \frac{1}{2}$, which means that the linear relationship between slope and intercept is most accurate when *Vp/Vs* is near *2.0*. In particular, for *Vp/Vs* greater than two there is considerable scatter from the trend that is unrelated to changes in *Vp/Vs*.

Consequently, AVO methods, which use distance from a background trend to detect hydrocarbons, are often more effective in deeper sediments where the background *Vp/Vs* ratio is close to 2.0 than shallow sediments where the *Vp/Vs* ratio is much greater than 2.0. Intercept or normal

incidence reflectivity can be a better hydrocarbon indicator in shallow unconsolidated sands than an AVO anomaly. Note that a Class III or IV gas sand will produce a large intercept or normal incidence reflection coefficient. (Polarity is important in this case.)

The second difference between (5) and (7) is the perturbation term with $\Delta\gamma$. Equation (7) implies that trends due to changes in γ or *Vp/Vs* are not symmetric with respect to the Fluid Line. If all other factors are equal, base of sand reflections lie farther from the Fluid Line trend than top of sand reflections. Although symmetric with respect to normal incidence reflectivity, Equation (7) predicts that the AVO response from the base of sand should be more prominent than the AVO response from the top of sand. Actually, it is fortunate that base of sand reflections have this enhanced AVO response because base of sand reflections can be used to identify fluid contacts or down-dip limits that provide further support for the presence of hydrocarbons.

Effects of Rock Property Changes on AVO

Up to this point, we have considered the effects of changes in elastic properties such as acoustic impedance and *Vp/Vs* on the seismic AVO response. The more important issue is the effect of changes in rock properties on the AVO response.

One property that has a significant effect on the AVO response is pore fluid compressibility. Gassmann's Equations (White, 1983, p. 60) predict the effect of pore fluid compressibility on the elastic properties of a porous, fluid-filled rock. Replacing brine with a highly compressible pore fluid like gas or light oil reduces the compressional wave velocity of the rock. Shear modulus is unaffected by the type of pore fluid. Thus shear wave velocity slightly increases because of the lower density of hydrocarbons. Consequently, increasing pore fluid compressibility significantly reduces the *Vp/Vs* ratio of the rock. Both (5) and (7) show that an abrupt change in the *Vp/Vs* ratio displaces the AVO response away from the Fluid Line trend by an amount dependent on the *Vp/Vs* contrast. The magnitude of the displacement from the Fluid Line increases as pore fluid compressibility increases.

The effect of pore fluid compressibility on AVO responses is depicted in Figure 2. The effect is similar to the results obtained by Batzle, Han, and Castagna (1995) for various pore fluids, including 20 API oil, 50 API live oil, and gas. They showed that gas, with the highest compressibility, produced the greatest departure from the Fluid Line trend, followed by 50 API live oil. Heavier oils with low gas content approach the response of brine saturated sands.

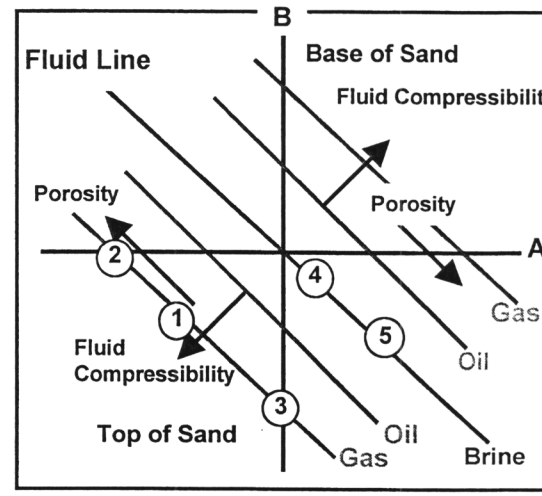

Figure 2. Effects of Porosity and Fluid Compressibility on the AVO response.

Porosity is another rock property that has a significant effect on seismic response. An increase in porosity decreases compressional wave velocity and density. Unlike fluid compressibility, which has little affect on shear wave velocity, an increase in porosity also decreases shear wave velocity. The decrease in shear wave velocity can offset the decrease in compressional wave velocity so that the *Vp/Vs* ratio is unchanged. Brie, et al. (1995), for example, reported a *Vp/Vs* ratio of 1.58 for clean gas sands, irrespective of porosity.

The effects of porosity changes on the AVO response are shown in Figure 2. Since increasing the porosity of a gas sand reduces its acoustic impedance, the intercept (A) of a reflection from the top of the sand becomes more negative and moves to the right in Figure 2. However, since porosity changes don't affect the *Vp/Vs* contrast, the slope-intercept value of the reflection must remain on a trend defined by the initial *Vp/Vs* contrast.

To illustrate how porosity affects the AVO response of a seismic reflection, suppose we observe a reflection from the top of a Class III gas sand designated by the point "1" in Figure 2. At normal incidence, the reflection from this Class III gas sand is negative and becomes more negative with increasing offset.

If we increase the porosity of this gas sand, its AVO response will move in the direction of the arrow in Figure 2, to the point "2". Moving to the point "2" makes the slope B more positive but decreases the intercept A. The reflection is larger in magnitude (more negative) but has less variation with offset than the reflection at "1". The reflection will appear as a "bright spot" on true-amplitude processed data.

Alternatively, if we reduce the porosity of the gas sand, we will move toward the point "3" on the cross plot in Figure 2. The resulting reflection will have a small amplitude at normal incidence, but its amplitude will increase in magnitude (become more negative) with increasing offset. The amplitude increase with offset is greater at "3" than at "1" or "2".

The reflection at the point "4" results from replacing gas with brine. This reflection will have a weak amplitude on a Fluid Line display, which measures deviation from the Fluid Line trend. Reducing the porosity of the brine will move the reflection from "4" to "5" on the cross plot in Figure 2. The reflection at "5" will be large and positive at zero offset, and its amplitude will decrease in magnitude with increasing offset.

Conclusions

Exact expressions for intercept and slope show that the Fluid Line trend has the least scatter when *Vp/Vs* is 2, and reflections from base of sands are more prominent than top of sand reflections. Slope and intercept cross plots are useful for interpreting AVO anomalies and explaining the effects of changes in rock and pore fluid properties.

References

Achenbach, J. D. 1973, *Wave Propagation in Elastic Solids*, North-Holland Publishing Co., Amsterdam.

Aki, K. and Richards, P.G., 1980, *Quantitative Seismology: Theory and Methods, Volume I*, W.H. Freeman and Co. San Francisco.

White, J.E., 1983, *Underground Sound – Application of Seismic Waves*, Elsevier Science Publishing Co. Inc., New York, NY.

Batzle, M.L, Han, D., and Castagna, J.P., 1995, Fluid effects on bright spot and AVO analysis, 65th Ann. Internat. Mtg., Soc. Explore. Geophys., Expanded Abstracts, 1119.

Brie, A., Pampuri, F., Marsala, A.F., Meazza, O., 1995, Shear sonic interpretation in gas-bearing sands, SPE Ann. Tech. Conf., Houston, TX.

Castagna, J.P. and Swan, H.W., 1997, Principles of AVO crossplotting: The Leading Edge, v.116, no. 4, pp. 337-342.

Castagna, J.P., Swan, H.W., and Foster, D. J., 1998, Framework for AVO gradient and intercept interpretation: Geophysics, **63**, 948-956.

Foster, D.J., Keys, R.G., and Schmitt, D.P., 1997, Detecting subsurface hydrocarbons with elastic wavefields, in Chavent, G., Papanicolaou, G., Sacks, P. and Symes, W., Eds., *Inverse Problems in Wave Propagation*: Springer-Verlag, New York.

Keys, R.G., and Foster, D.J., Eds., 1998, *Comparison of Seismic Inversion Methods on a Single Real Data Set*, SEG Open File Publication.

Rutherford, S.R. and Williams, R.H., 1989, Amplitude-versus-offset variations in gas sands: Geophysics, 54,680-688.

Shuey, R. T., 1985, A simplification of the Zoeppritz equations: Geophysics, **50**, 609-614.

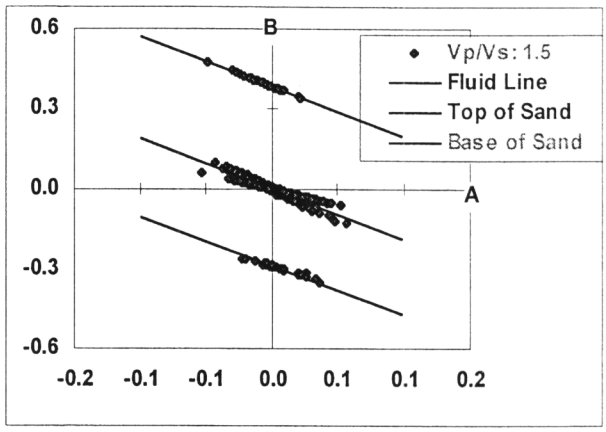

Figure 3. Predicted Trends from (7) vs. Slope and Intercept Values from sonic and density logs from Well A, (Keys and Foster, 1998). Shear wave velocities were derived by using Vp/Vs=1.9 in background rocks and 1.5 in sands.